We are IntechOpen, the world's leading publisher of Open Access books Built by scientists, for scientists

4,800
Open access books available

122,000
International authors and editors

135M
Downloads

Our authors are among the

154
Countries delivered to

TOP 1%
most cited scientists

12.2%
Contributors from top 500 universities

CLARIVATE ANALYTICS BOOK CITATION INDEX INDEXED

WEB OF SCIENCE™

Selection of our books indexed in the Book Citation Index in Web of Science™ Core Collection (BKCI)

Interested in publishing with us?
Contact book.department@intechopen.com

Numbers displayed above are based on latest data collected.
For more information visit www.intechopen.com

Chapter 4

The New Generation of Diamond Wheels with Vitrified (Ceramic) Bonds

Barbara Staniewicz-Brudnik, Elżbieta Bączek and Grzegorz Skrabalak

Additional information is available at the end of the chapter

http://dx.doi.org/10.5772/59503

1. Introduction

Modern, composite materials: non-ferrous metal alloys reinforced with hard particles, wood composites, plastic composites reinforced with glass fibers, nickel super-alloys (Hastalloy, Waspalloy, Inconel 718, Udimet720) and titanium Ti6Al4V, TiAl) [1-5] requires the development of technology taking into account abrasive tools with new binders [6-9].It is emphasized that provided affective work tools in the optimal adjustment of the characteristics of grinding machines, machining parameters, the characteristic of tools and a method of cooling and dressing. Typical bonded abrasive tool includes: super hard grains (diamond cubic boron nitride, mono-or microcrystalline microstructure), filler(corundum, silicon carbide, boron nitride etc.), binder (sintered metal, electroplated, resin, ceramic, hybrid), modifiers (homogenizers, greases), body (metal, ceramic, polymer). Currently as bonded abrasive products are mainly used synthetic diamond or cubic boron nitride grains. Significant diamond grains producers were shown in table 1 [10]

Producer	Trade name of diamond	Grains morphology	Application
Sandvic Hyperion, USA	MBG 600	Irregular, sharp, friable	Coarse and fine grinding ceramics, glass and precious
	MBG 640	Cubooctahedral crystals with high impact and fracture strength, free cutting capability	

Producer	Trade name of diamond	Grains morphology	Application
	RVG	Irregular shapes, medium friable crystals	Precision grinding and finishing of tungsten carbide and carbide, grinding of
	RVG 800	Irregular shape, superior free capabilities due to controlled micro fracturing mode of crystals	
	RBI - uncoated	Irregular shape, medium friable crystals	grinding of tungsten carbides and PCD inserts
	SPR	Uncoated economic grade grain, the friability of SPR enables controlled diamond fracturing, wheel self-sharpening and free cutting action	
Element Six, USA	PDA 657		It is suited for used in less applications where sharp cutting characteristic are important
	PDA 321 PDA 311 PDA 211	microchipping structure, friable	Grinding of cermets and elements of technical ceramic
Gems Superabrasives, China	GRD 10 GRD 20	Multi crystal shape, consisting of many micro crystals with slight friability enable excellent self- sharpness	Grinding of soft Stones cutting,, sharpening, grinding ceramics and rubber
Lands, USA	LS 070	Ultra friable, irregular shape	Specialized grinding benefiting from free cutting crystals
	LS 100	Friable, irregular shape	
	LS 600F	Uniform, blocky friable	Grinding lapping, polishing of cemented carbide, special steels, glass, natural stone
Kingray New Materials & Science Technology Co., China	JRI – typ A JRI – typ B	irregular shape	Grinding of nonferrous hard alloys
Changha 3 better ultra HARD MATERIALS, China	SMD 690	Premium grade grain with high strength and great thermal stability	
	MBD 6 MBD 4	Sharp crystal shape	Grinding stones ,ceramics, polishing of hard materials optical glass grinding
	RVD	Irregular crystal shape preferably self-sharpness	Grinding of hard alloy, non-ferrous metal, polishing of natural diamond
	RVE	Friable and strong self-sharpness, policrystallic shape, low hardness	Fine processing ceramics, optical glasses, grinding, polishing of

http://dx.doi.org/10.5772/59503

Producer	Trade name of diamond	Grains morphology	Application
			nonferrous metals and nonmetallic materials, PCD, carbide, granite
SF Diamond, China	SFD 10	Irregular shape, rough surface low strength	For grinding tools, which work with low load
	SFD 20 SFD 30	Irregular crystal shape, rough surface, low strength	
	SFD 40 SFD 50	Comparatively regular crystal shape, medium strength	For grinding wheels, which work with medium and low load
	SDM-c	Dark green color, medium tough, micro-friable multinano crystal, irregular shape, perfect self-sharpen ability	
The Institute of Super Hard Materials Kiev Ukraine	AC 4 AC 6	Irregular shape, friable, low strength	Grinding of brittle materials (ceramic, hard alloys, glass)
	AC 15 AC 30	Irregular shape, less friable, medium strength	
	AC 100 ACR	Comparatively regular crystal shape, medium strength	

Table 1. Significant producers of diamond grains

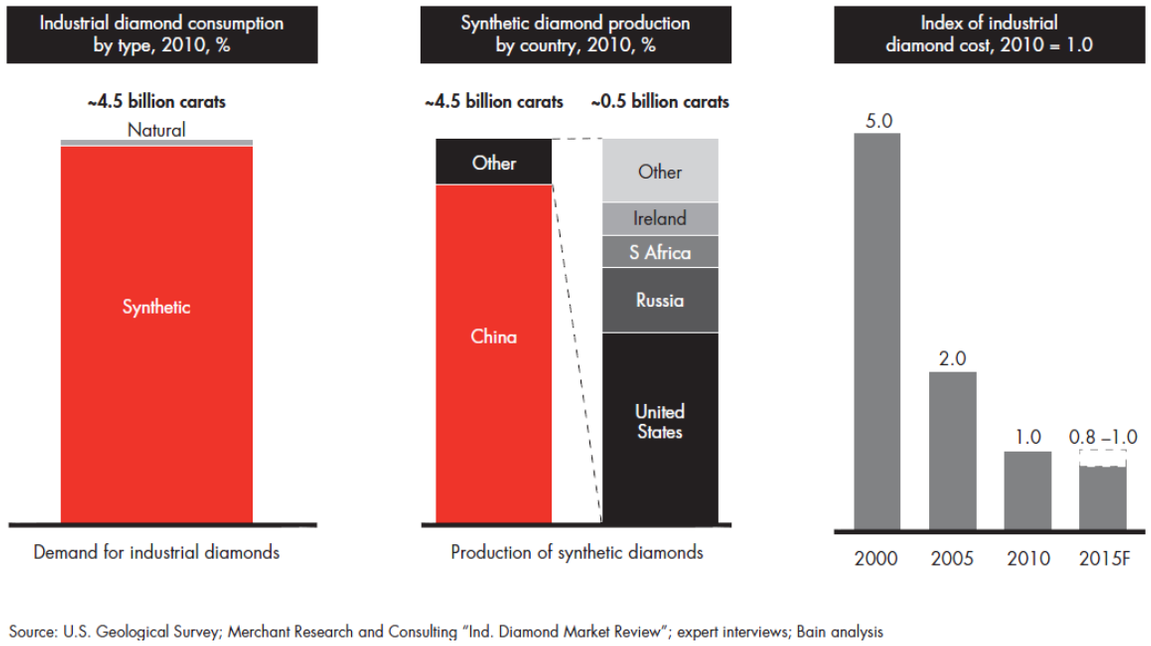

Figure 1. Synthetic industrial diamonds production [1]

In general, monocrystalline grains, used for tools with vitrified bond are assigned for grinding of flat and shaped surfaces, for example grinding of internal surfaces of Titan alloys and sharpening (fig. 2). Microcrystalline grains are complexes consisting of collection of small microcrystals with sizes ranging from one to a few microns, characterized by a higher mechanical strength, and higher ductility of monocrystalline grains (fig. 3)

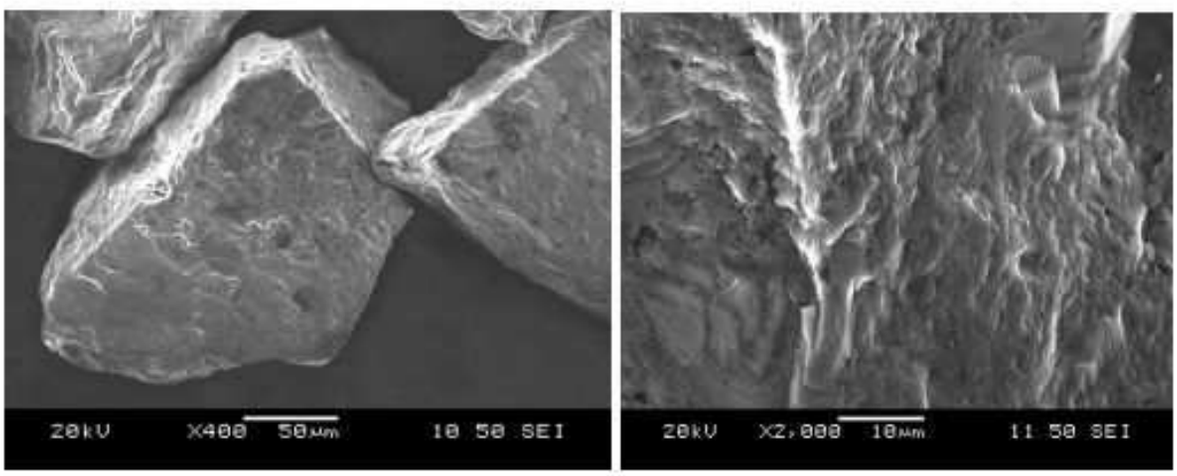

Figure 2. Microcrystalline diamond grains magn.: a) 400x, b) 2000x

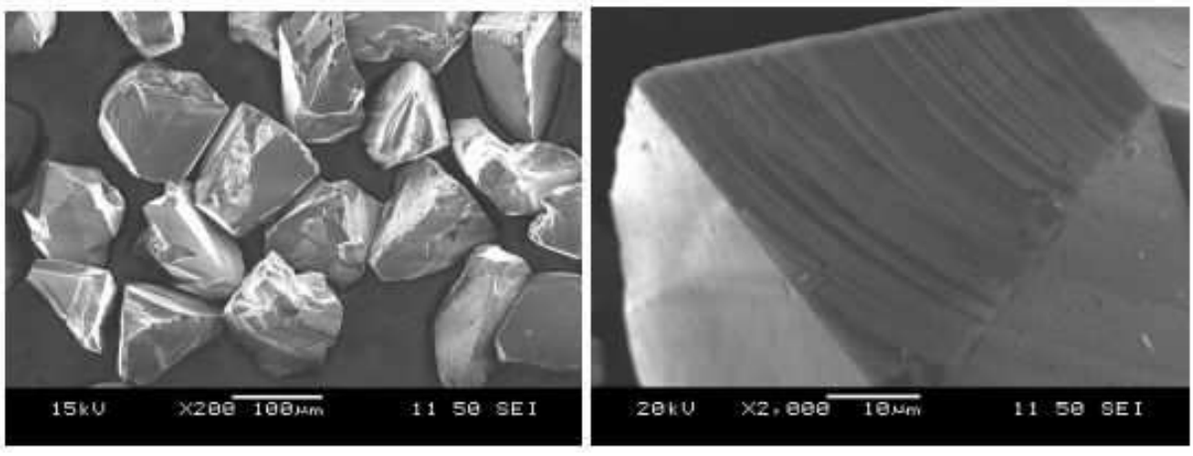

Figure 3. Monocrystalline diamond grains magn.: a) 200x, b) 2000

The microcrystalline grains are recommended for grinding operations, where surface quality is the main processing criterion. The fillers can be alumina, silicon carbide, tungsten, zirconium silicate etc. It is assumed that the filler, introduced into the binder, protects the seed prior to the dynamic action of chips (typically having a higher temperature) and that increases the strength properties of the sinter, the thermal resistance and wear resistance, also taking part

http://dx.doi.org/10.5772/59503

in the grinding process. The binder is a factor connecting the embankment of grain in the wheel causes the maintenance work until the grains have sharp edges, thereby induced on the self-sharpening effect of the grain. The efficiency of binders application provide features such as adequate strength of fixing force of particles in the binder, wear resistance, the possibility of sintering of the tools below temperature of graphitization (diamond) or active oxidation (CBN), having long thermal conductivity allowing for intense heat removing from the grinding zone without accumulation, the coefficient of thermal expansion close or identical with the coefficient of thermal expansion of the abrasive grain, proper hardness and strength, no reaction with work-piece material [6-8, 11-13]. Vitrified binders are primarily glass or devitrificate from the multicomponent system, received from synthetic chemicals with very high purity [6, 9].

They are divided into a low-melting binder (sintering temperature up to 730^{o} C), medium (sintering temperature up to 880^{o}C) and a high-melting (sintering temperature above 900^{o}C). The most characteristic systems are borosilicate glasses modified with various oxides (Na_20, Li_20), calcium-silicate glasses, modified by V_20_5, Fe_20_3 or P_20_5, lead-borosilicate devitrificates, barium-borosilicate with the addition of bismuth oxide. The most famous research centers dealing with binders for super hard tools including vitrified bond are located in Worceaster (GE company-USA), Aachen(RWTH-Germany), Sankt Petersburg (Ilyich company –Russia), Kiev (Institute of Super hard Materials –Ukraine), Zhengzhou (Zhengzhou Concern Hongtuo Superabrasive Products Co.-China). The Institute of Advanced Manufacturing Technology is conducting researches aiming at obtaining ceramic binders for super abrasives tools with controlled physical and mechanical properties and testing tools containing these binders. This publication shows the results of research of new vitrified (ceramic) binders and testing of grinding tools with these binders for the latest generation of composite BNDCC (boron nitride dispersive in cemented carbide) of various grit size of cubic boron nitride grains.

2. Experimental section

2.1. Part I Preparation and study of some physical and mechanical properties of glasses

2.1.1. The starting materials and methods of research

The study selected five variants of glasses from the $Si0_2$-Al_20_3-B_20_3-Na_20-Ba0 system. The following were used as starting materials:

- silicon dioxde -$Si0_2$ pure
- hydrated aluminum nitrate Al $(N0_3)_3$ x9H_20 of high purity or aluminum hydroxide Al $(0H)_3$
- barium carbonate $BaC0_3$-pure
- boric acid H_3B0_3-pure
- sodium carbonate Na_2C0_3-pure

After accurate grinding, sieving through a 0.63mm sieve and mixed, raw materials were placed in corundum crucibles and heated at a temperature above 1,350° C. After fritting (hot melt glass pouring into cold water) and once again the glass was milled and sieved. All glass frits were completely transparent with bluish color. On the received materials the following tests were carried out:

- the density of helium, on Accu Pyc II 1340V10 helium pycnometer using 5 parallel samples;
- the X-ray diffractometer of Panalytical Empiriam with copper lamp in the range of 2 theta angle of 5 to 90 degrees;
- calculation of thermodynamic stability using algorithm VCS for sets of glasses in temperatures of 700, 900, 1300 and 1500° C on two assumptions: the total miscibility of liquid and vapor phases or total immiscibility liquid and vapor phases;
- the reactivity of raw materials of glasses and the melt glasses using differential scanning calorimetry (DSC-device STA-449 F3 Jupiter)
- the wettability of glasses to the substrate of silicon carbide or sintered alumina (cubitron) on the high-temperature microscope of Leitz -Watzler type by sessile-drop method.
- microscopic observation (SEM)of transverse specimens after testing the wettability
- the Young's modulus of glass using a flaw with the head broadband
- the three-point bending strength of trabecular glass, describing the work of destruction by using a machine Zwick Roell Z2.5

2.1.2. Results and discussion

Test glass belonged to the group of light, characterized by a low density, ranging between 2.34 (W4), and 2.69 g/cm^3 (Ba23bis). It was evident that with the reduction of silicon dioxide content in the glass, decreasing the density of the glass increased A slight increase in the content of barium oxide, the constant of silicon dioxide and reduced alumina content did not affect significantly the increase in density. The results are summarized in Table 2

The variant of glasses	Density [g/cm^3]
W1	2,4548
W2	2,5347
W3	2,4320
W4	2,3426
Ba 23 bis	2,6912

Table 2. The density of the tested glasses

http://dx.doi.org/10.5772/59503

2.1.3. Calculations of thermodynamic stability of the glasses by algorithm VCS

Chemical stability of the connections between components of the glasses was determined by calculation of the thermodynamic potential of components by VCS algorithm, which takes into account the probable stability of the reaction products. Equilibria calculations were performed for the four variants of the glasses of the SiO_2-Al_2O_3-BaO-B_2O_3-Na_2O system in temperatures 700° C, 900° C, 1,350° C, 1500° C at atmospheric pressure 1013 hPa. The molar ratios of the components were adopted taking into account their actual values. It was assumed that the component of glass within these ranges of temperatures may occur: in a multicomponent gas phase and condensed phase pure (liquid and solid). It is not known whether the active phase pure liquid form (that are immiscible with each other) or a liquid phase formed of unlimited miscibility, therefore, the calculation was performed by two assumptions out. Of the approximately 100 likely stable compounds there were 10, of which the solid 3. Summary of solid stable compounds glass as an example of option 2 are shown in Tables 3 and 4.

Name of compounds in solid phase	700° C	900° C	1350 ° C	1500 ° C
$NaAlSi_3O_8$	0,9096	0,92326	–	–
$Al_4B_2O_9$	0,0772	0,0430	–	–
$Al_6BSi_2O_{13}$	–	–	0,15674	0,15674
$BaSi_2O_5$	–	–	0,08201	0,08201
SiO_2	–	–	2,4153	2,4153

Table 3. Calculation of the thermodynamic stability of glass precursors, option 1 assumption 1

According with the first assumption at high temperatures (1350, 1500° C) there should be stable three compounds: an aluminum borosilicate ($Al_6BSi_2O_{13}$), barium silicate ($BaSi_2O_5$) and silicon dioxide (SiO_2). In the second assumption the second barium silicate ($BaSi_2O_5$) presented only one. Similarly were in the other glasses. The verification of the existence of these compounds in the glass was carried out on the basis of X-ray examination.

Name of compounds in solid phase	700°C	900°C	1350°C	1500°C
$NaAlSi_3O_8$ c.s	0.89295	0.86483	–	–
$Al_4B_2O_9$ c.s	0.01188	0.01891	–	–
$Al_6BSi_2O_{13}$ c.s	–	–	0.15674	0.15674

Table 4. Calculation of the thermodynamic stability of glass precursors, option 1 assumption 2

2.1.4. X-ray research of the glasses

The study of X-ray glasses clearly showed amorphous structure, as evidenced increase in the background at low angles and lack of educated, sharp peaks throughout the angular range.

(fig. 4-X-ray glasses of W1). The existence of crystalline barium silicate ($Al_6BSi_2O_{13}$) was not found.

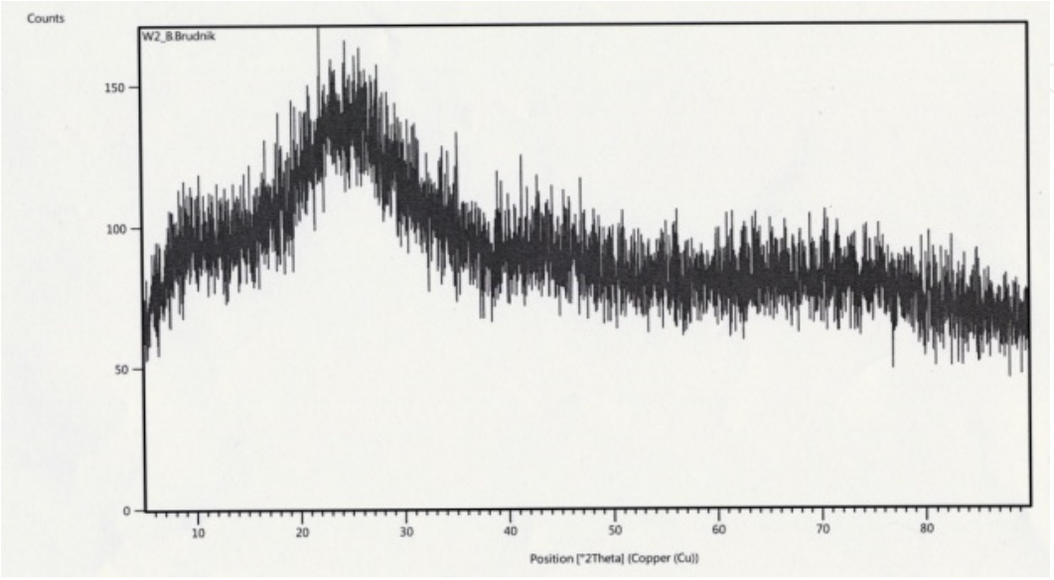

Figure 4. An example of X-ray glass, variant W1

2.1.5. Differential scanning calorimetry research

Thermal analysis of the five types of the glass raw materials and glass of W1 variant was based on differential scanning calorimetry. This method consisted of recording energy required to bring to zero the difference in temperature of the test sample and the reference material as a function of temperature or time.[14] The shape of the DSC curve showed a good agreement with the DTA curve. Endothermic peak was created when the sample temperature was below the standard, and the exothermic peak, when the temperature of the sample was higher than the reference. Samples containing a mixture of raw materials (precursors) of glass heated at a rate of 5° C/min to a temperature of 1400° C. When analyzing the plots, it can be concluded that the incomplete decomposition of the raw materials with the separation of water or CO_2 to a temperature of 350°C occurred, as reflected by the different endothermic peaks. The earliest release of the water of hydration of aluminum nitrate (variant W2-71,0° C, 80,0° C), followed by water coming from the decomposition of boric acid (W1-127,3° C) and CO_2 from the decomposition of sodium carbonate. At a temperature of 548° C on curves of W2 and Ba23 bis inflection appeared to indicate polymorphic transitions of silicon dioxide with the appearance of high gamma phase. For all graphs at about 1230° C and above the melting peak of barium carbonate was observed. Full homogenization mixture of precursors occurred above 1,350° C (W1-DSC chart in fig. 5 and 6)

http://dx.doi.org/10.5772/59503

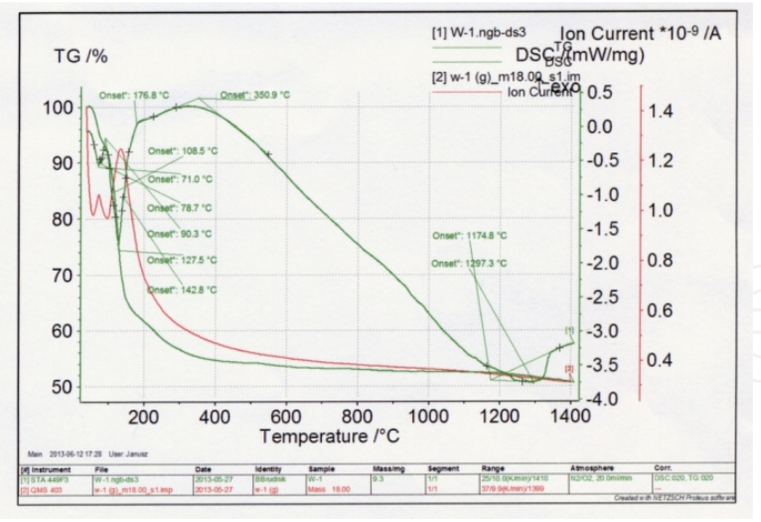

Figure 5. DSC curves of glass raw materials, variant W1

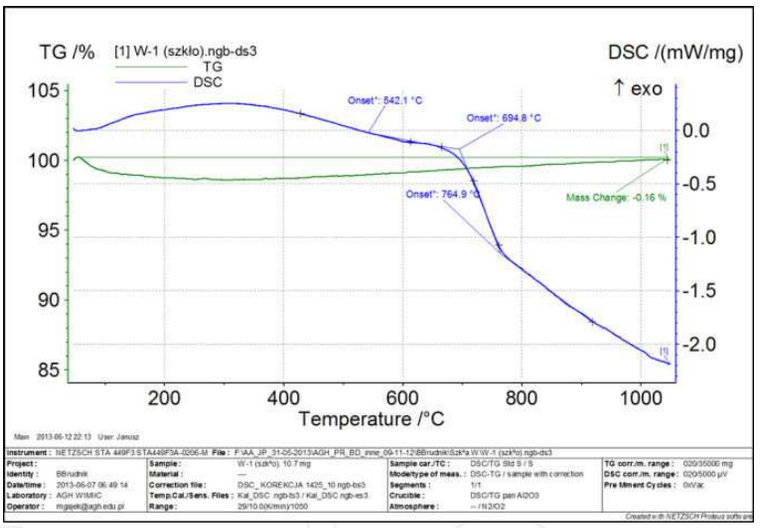

Figure 6. DSC curves of glass, variant W1

Analyzing the DSC plot of W1 glass could be seen of his amorphous. The inflection of the curve reported that there was at 542°C vitrification and 649,8°C started the process of softening. On the thermogravimetric curve TG were not visible weight loss upon heating the glass.

2.1.6. Wettability research of glasses

The study of wettability of glasses to substrates of silicon carbide or submicrocrystalline sintered corundum is performed using high-temperature microscope of Leitz- Watzler, type using sessile drop method. Silicon carbide is used as a filler in diamond grinding wheels or supporting grain. SiC substrate, there was degassed under vacuum, and therefore contain adsorbed gases from the air (oxygen, nitrogen), and chronic alcohol bath defatted not entirely

surface. Therefore, the observed high temperature sintering (for all variants within 620-670° C glasses) and the temperature drops propagation (920-970° C).

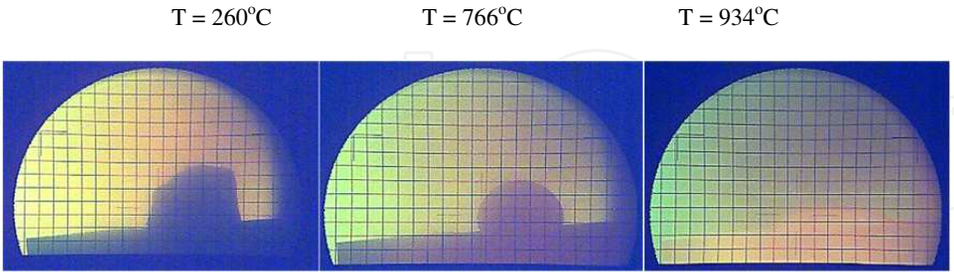

Figure 7. Wetting of cubitron substrate by glass, W1 variant

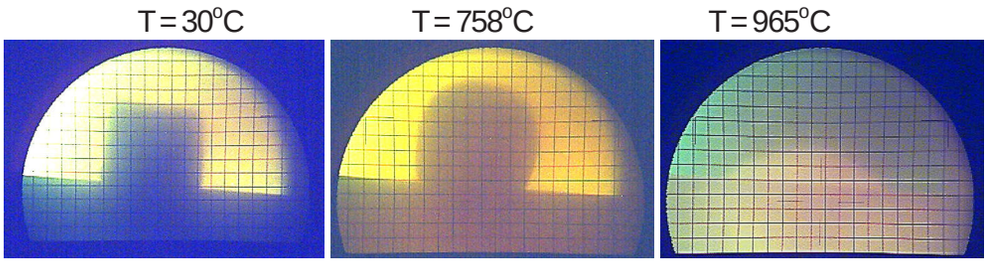

Figure 8. Wetting of silicon carbide substrate by glass, W1 variant

Contact angle theta ranged less than 40 degrees. All the tested glass wetted submicrocrystalline sintered corundum (cubitron) substrate better than the silicon carbide substrate, at lower temperatures (880-930° C), although the same procedure of degreasing were conducted.

2.1.7. Mapping of the surface of glass-substrate microsection

Microscopic observation of transverse cross-sectional views of the glass –SiC substrate or glass-submicrocrystalline sintered corundum substrate carried out using a scanning electron microscope JSM 6460LV and starters EDS (Energy – dispersive X-ray spectroscopy analyzer) revealed the presence of a small transition layer in the system glass- submicrocrystalline sintered corundum (pictures of the glass Ba23 bis-submicrocrystalline sintered corundum) contains barium elements. The phenomena of interlayer (fig. 9) in the case of specimens glass-silicon carbide substrate comprising this was much wider probably resulted from the presence of silicon, both in the glass and substrate.

http://dx.doi.org/10.5772/59503

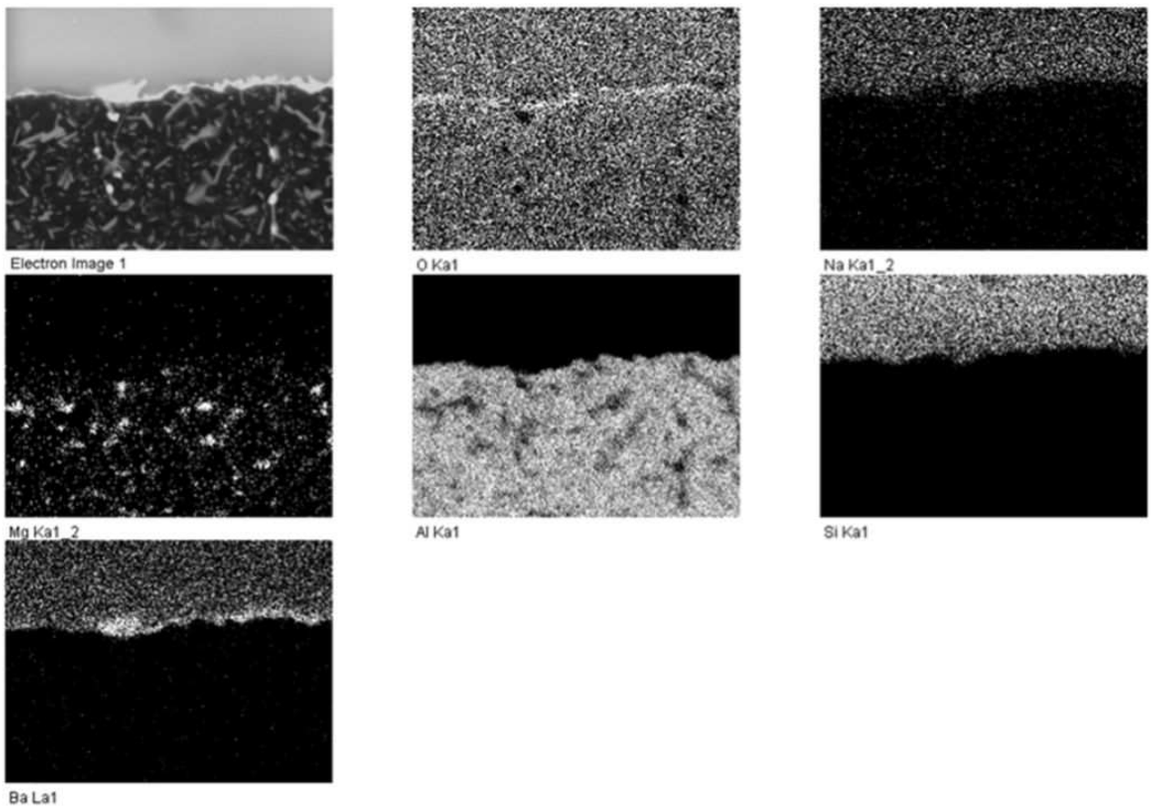

Figure 9. Picture of mapping of the surface of glass-substrate microsection – Ba23 bis variant

2.1.8. Testing the strength of glass

Flexural testing was performed on the four groups of glasses for Zwick Roell Z2.5 machine, at the test speed of 0.5 mm/min, and the spacing supports 34 mm The flexural modulus was determined for all samples by the secant, taking reference points as a force of 50 N and 100 N start the end (Table 5). Maximum bending strength in the range of 100 MPa was obtained for the samples of glass W1 and Ba23 bis. For a group of glasses W4 and W3 it was lower by half. This can be explained by the reduced content of primarily silicon dioxide in these glasses. Similar behavior was observed in the samples of the destruction operation. The largest value of the work of destruction (W1-19,27 N/mm) was obtained for samples W1 and three times lower for samples W3.

Names of samples	Bending strength [MPa] average value	Work of destruction [N/mm] average value	Bending modulus [GPa] average value
W1 glass	105,72 +-2	19.27	25,945
W3 glass	87,08	17,31	14,141
W4 glass	52,29	5,62	21,418
Ba23 bis glass	101,35	16,49	27,195

Table 5. Measurement of flexural strength of glass

2.1.9. Young modulus measurement of glasses

The measurements were carried out on the test bench equipped with a flaw, heads broadband and a PC with installed software. Young's modulus and Poisson's ratio of the samples based on the determined velocity of the longitudinal wave and transverse density of the material. All calculations were performed using the program Modulus 1.0. The highest values obtained of glass Ba23 bis (87 GPa) (Table 6). Poisson's ratio for all glasses were the same (0.38).

Name of samples	Poisson's ratio	Young modulus [GPa]	Modulus uncertenainty [%]
W1 glass	0.38	79	2,2
W3 glass	0.38	79	2,2
W4 glass	0.38	76	6,2
Ba 23 bis glass	0.38	87	5,8

Table 6. Measurement results of Young modulus

2.2. Part II Operational tests of grinding wheels containing the newly developed glass

2.2.1. The starting materials and methods of research

After summarizing the results of studies on the physical and mechanical properties of the newly developed glass, two of them with the best value properties (Ba23 bis and W1) were selected and used to develop the recipe wheel. Test wheels were prepared to carry out grinding tests. Grinding of flank surface of BNDCC composite samples was performed using wheels 6A2 100x10x4 mm type, containing uncoated diamond grain, Lands LS120 (D46-45-38 microns) type or LS 600F (D25-20-30 microns) with higher concentration of diamond (C125%) and a W1 or Ba23 bis binder (Fig. 9b).

Using DOE, influence on surface roughness and process efficiency of following parameters was derived:

- grinding wheel peripheral speed, v_s = 12, 15, 20 m / s
- working engagement $a_{e:}$ 0.002, 0.005, 0.01 mm / double stroke of the table
- diamond grain D46, D25

Constant parameters during experiments were:

- a research position with the universal tool grinder 3E642,
- the characteristics and dimensions of the grinding type 6A2 100x10x4 mm
- the type of coolant-fed Synkom PGA
- the method by pouring coolant

http://dx.doi.org/10.5772/59503

- maschining time of the one cycle, t = 600 s,
- number of the table double strokes – 3
- table feed speed, v_f = 210 mm / min
- BNDCC composites

The study was carried out on a modernized grinding universal tool grinder 3E642 (fig. 10a), equipped with stepless speed control of the wheel and the cooling system. Grinding process was carried out with cooling by spraying a 2% solution of PGA Synkon coolant concentrate in tap water.

To test of the efficiency of grinding process of custom BNDCC composite sample (boron nitride dispersive in cemented carbide), comprising weight 20% of the grains of cubic boron nitride, with granulation 4-8 mm and dimensions 19x5,7 mm from the edge intersected at a distance of 1 mm from the end, were made at the Warsaw Univeristy of Technology, at the Faculty of Materials Science and Engineering. Before attempts to work the sample was adhered to the brackets in order to attach them to the machine (fig. 10c). Below the picture shows the position of the test, the wheel and bonded composites (fig. 10b).

a) b) c)

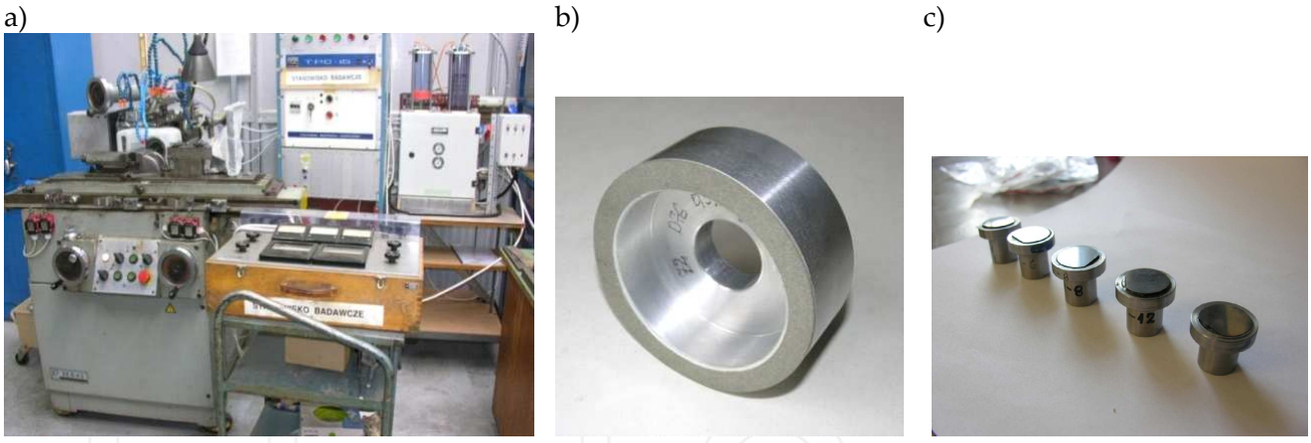

Figure 10. a) The position of a universal tool grinder 3E642 grinding tests with cooling, b) diamond grinding wheel vitrified Ba23 bis c) composites BNDCC intended for research

Measured: the height of abraded material m, height of wheel. Calculated: the volume of abraded material Vw, consumption volume Vs wheel, radial wheel wear Vrs, grinding ratio G, yield losses of (volumetric) Qw, proper performance defects Q'w (deficient performance attributable on the active wheel width).

Sample mass measurements were carried out before and after each treatment using a laboratory scale with an accuracy of measurement 0.001 g. Measurements of the height of wheels and work-before and after each test was performed using electronic calipers accurate to 0.01 mm.

For the measurement of surface topography work-pieces profiler workshop was used. Before and after test were performed via research work on modul profilometer TOPO 01vP designed for measurement and analysis of surface roughness and waviness profiles and the profile of the actual surface without filtration with the program PROFILE. Images of 2D, 3D, marked elevation values $R_{z,}$ $R_{t,}$ Ra and horizontal parameters W, St, Sa in accordance with PN-EN ISO 4287th were conducted. The microscopic observations (SEM) of the samples before and after grinding were made. The designated function of the object of research in the form of a polynomial of the second degree of interaction, allowed to determine the statistical relationship between the basic parameters of the treatment and its effects (surface roughness).

2.2.2. Results and discussion

The results of grinding tests of D46 diamond grinding wheels with newly developed binders worked at a peripheral speed of 12, 15, 20 m / s and depth of grinding 0.002, 0.005 mm/double stroke of the table. were presented in Tables 7-8 and figures (fig. 11-16). It was evident that both: the D46 Ba23 bis wheel andW1 D46 wheel were best operating at a depth of 0.005 mm grinding/double stroke. The uniform wear of diamond grains and their self-sharpening were demonstrated.

The grinding wheels with D25 grit size of diamond grains worked at a speed of 15m/s and depth of grinding 0.002 and 0.005 mm/double stroke. All the grinding performance parameters were comparable for both types of wheels. Better results were obtained by D25 grinding wheels with Ba23 bis binder. For the depth of the grinding process the surface roughness of machined BNDCC composites varied within the same limits 0.02-0.03 μm. Comparing the results of performance parameters of the process of grinding wheels with the D46 and D25 granulation can state that they were very similar. Slightly better results were obtained with the wheels with lower diamond grit size (D25).

Kind of wheel	Working engagement a_e, mm	Peripheral speed of wheel vs, m/s	Qw, x10^{-3} mm^3/s	Q'w, x10^{-3} mm^3/ mm·s	G [-]	R_a, μm
D46 W1	0,002	12	1,32	0,13	13,56	0,03
D46 Ba23 bis			1,35	0,14	3,41	0,03
D46 W1		15	2,30	0,23	31,12	0,03
D46 Ba23			2,29	0,23	29,48	0,03
D46 W1		20	1,19	0,12	12,02	0,03
D46 Ba23			1,31	0,13	17,91	0,03

Table 7. Results of performance parameters of the process of grinding the surface of composites BNDCC 3,14 D46 grinding wheel W1, Ba23 bis, v_s = 12, 15, 20 m/s with working engagement a_e = 0,002 mm

http://dx.doi.org/10.5772/59503

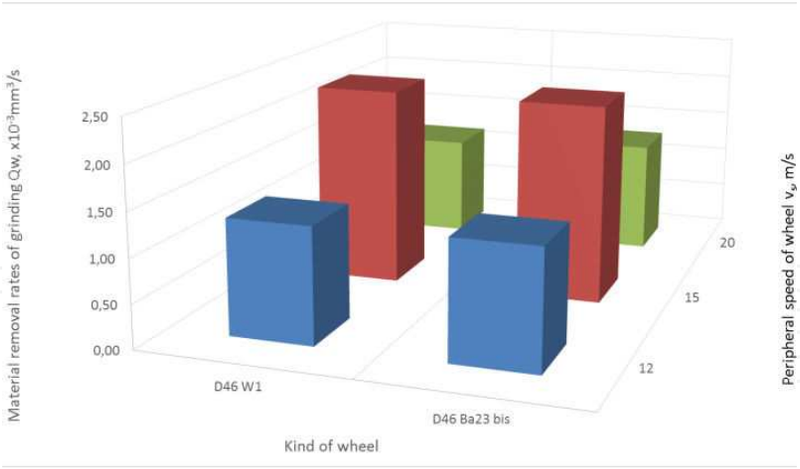

Figure 11. The diagram of material removal rate Qw, x10^{-3} mm^3/ s after grinding of the surface of composites BNDCC 3,14 samples with D46 W1 and Ba23 bis grinding wheels with working engagement a_e: 0.002 mm/double stroke of the table

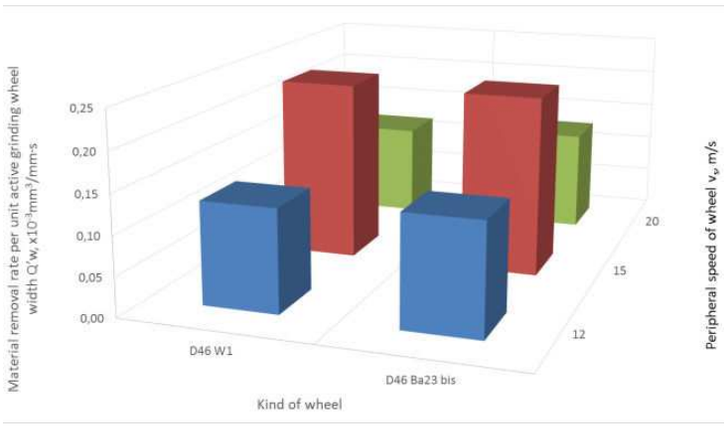

Figure 12. The diagram of material removal rate per unit active grinding wheel width Q'w, x10^{-3}mm^3/mm·s after grinding of the surface of of composites BNDCC 3,14 samples with D46 W1 and Ba23 bis grinding wheels with working engagement a_e: 0.002 mm/double stroke of the table

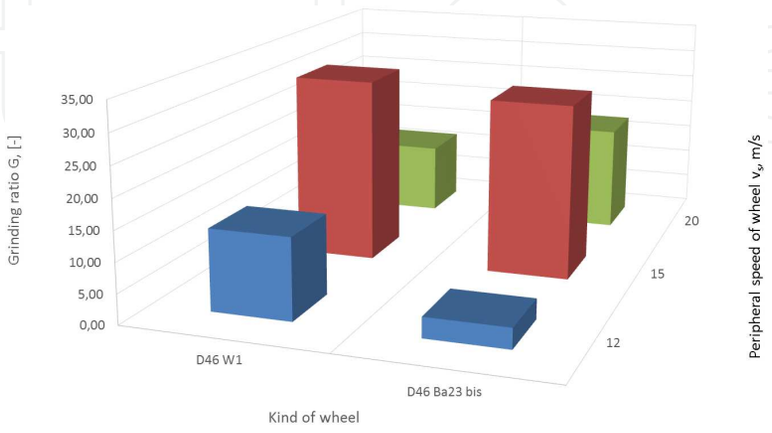

Figure 13. The diagram of grinding ratio G, mm^3/mm^3 for grinding wheels with working engagement ae 0.002 mm/ double stroke of the table

Kind of wheel	Working engagement a_e, mm	Peripheral speed of wheel vs, m/s	Qw, x10^{-3} mm^3/s	Q'w, x10^{-3} mm^3/mm·s	G	R_a, μm
D46 W1	0,005	12	1,24	0,12	17,39	0,03
D46 Ba23			1,27	0,13	5,88	0,03
D46 W1		15	2,25	0,23	15,24	0,03
D46 Ba23			2,23	0,22	26,94	0,03
D46 W1		20	1,13	0,11	7,82	0,02
D46 Ba23			1,21	0,12	16,94	0,03

Table 8. Results of performance parameters of the process of grinding the surface of composites BNDCC 3,14 D46 grinding wheel W1, Ba23 bis, v_s = 12, 15, 20 m /s with working engagement a_e = 0,005 mm

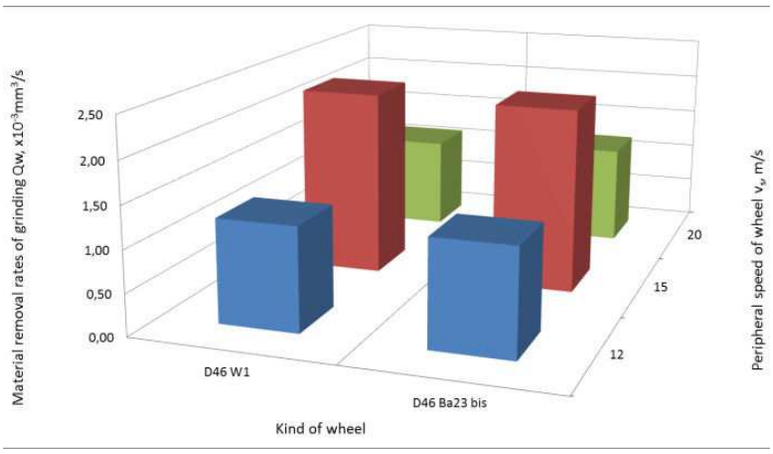

Figure 14. The diagram of material removal rate Qw, x10^{-3} mm^3/s after grinding of the surface of composites BNDCC 3,14 samples with D46 W1 and Ba23 bis grinding wheels with working engagement a_e: 0.005 mm/double stroke of the table

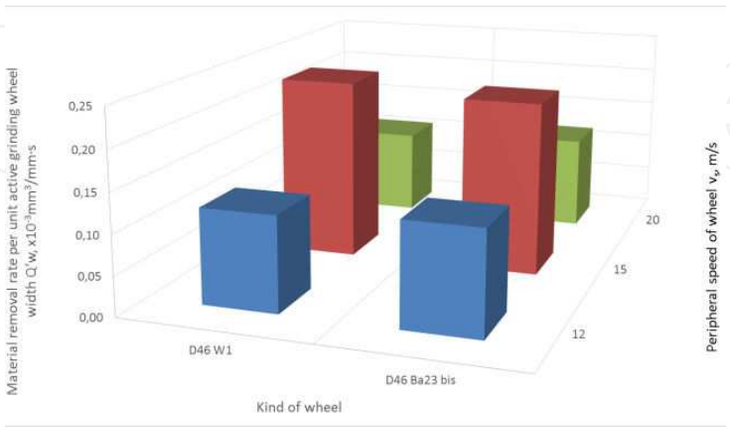

Figure 15. The diagram of material removal rate per unit active grinding wheel width Q'w, x10^{-3}mm^3/mm·s after grinding of the surface of composites BNDCC 3,14 samples with D46 W1 and Ba23 bis grinding wheels with working engagement a_e: 0.005 mm/double stroke of the table

http://dx.doi.org/10.5772/59503

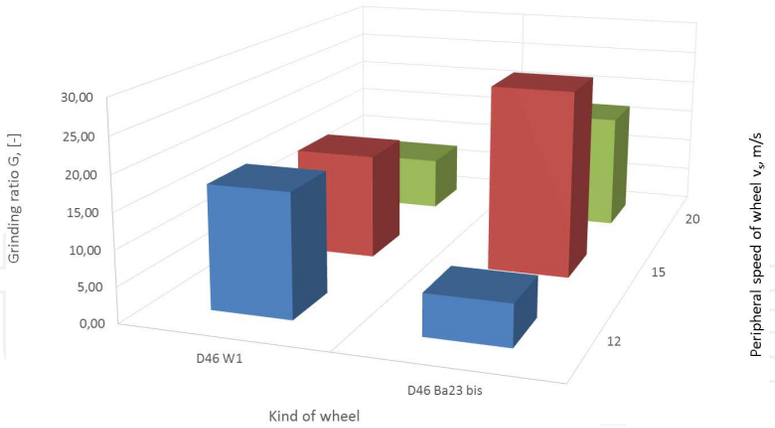

Figure 16. The diagram of grinding ratio G, mm^3/mm^3 for grinding wheels with working engagement ae 0.005 mm/ double stroke of the table

Kind of wheel	Working engagement a_e, mm	Peripheral speed of wheel vs, m/s	Qw, $x10^{-3}$ mm^3/s	Q'w, $x10^{-3}$ mm^3/ mm·s	G, [-]
D25 Ba23 bis	0,002	2,31	0,23	31,60	0,02
D25 W1		2,13	0,21	21,91	0,02
D25 Ba23 bis	0,005	2,22	0,22	27,65	0,03
D25 W1		2,02	0,20	27,08	0,02

Table 9. Results of performance parameters of the process of grinding the surface of composites BNDCC 3,13 D25 grinding wheel W1, Ba23 bis, v_s = 15 m/s

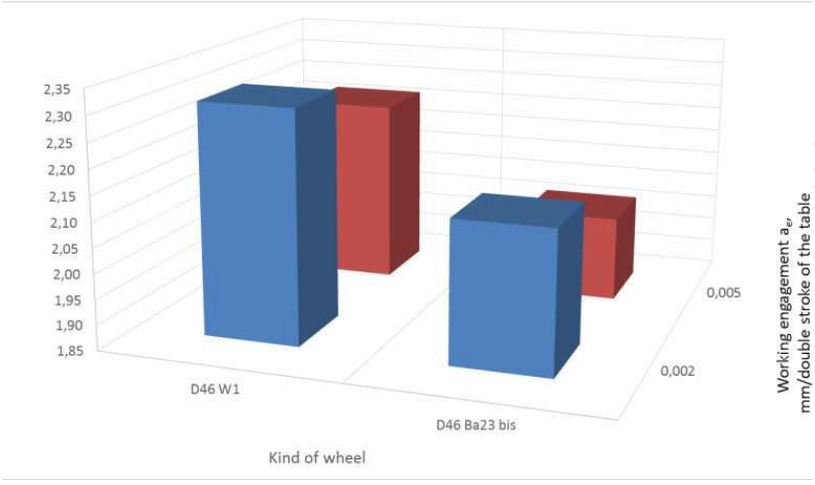

Figure 17. The diagram of material removal rate Qw, $x10^{-3}mm^3/s$ after grinding of the surface of composites BNDCC 3,13 samples with D25 W1 and Ba23 bis grinding wheels with working engagement a_e: 0.002, 0.005 mm/double stroke of the table

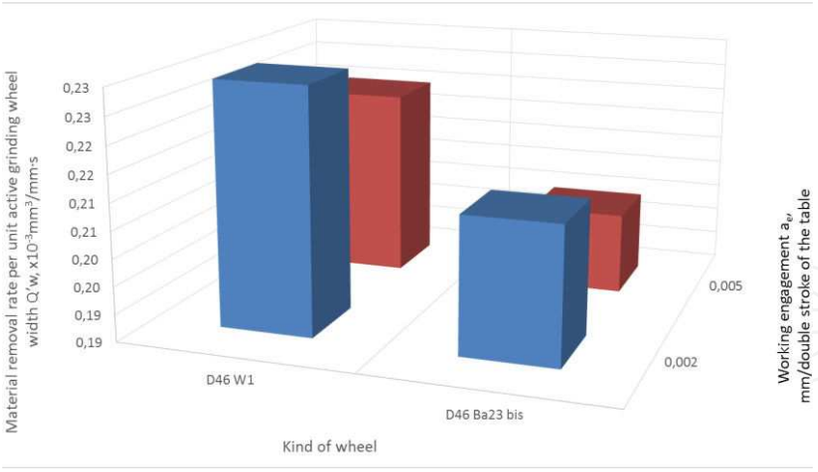

Figure 18. The diagram of material removal rate per unit active grinding wheel width Q'w, $x10^{-3}$ $mm^3/mm \cdot s$ after grinding of the surface of composites BNDCC 3,13 samples with D25 W1 and Ba23 bis grinding wheels with working engagement a_e: 0.002, 0.005 mm/double stroke of the table

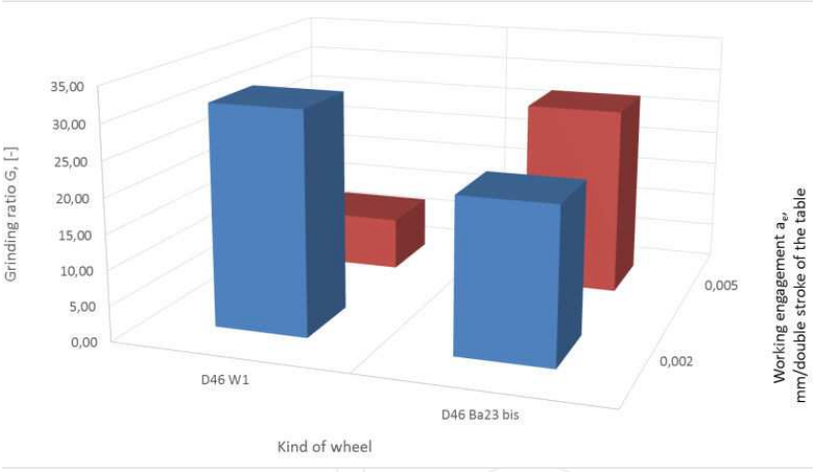

Figure 19. The diagram of grinding ratio G, mm^3/mm^3 for grinding wheels with working engagement ae 0.002 and 0.005 mm/double stroke of the table

2.2.3. Research of geometric structure of BNDCC composites

The study of geometric structure of the samples before and after grinding showed that the assumed test conditions are properly selected (Figure 20a). Machining by grinding the assumed operating parameters of wheel allowed to obtain roughness parameters (R_a, R_z, R_t) times better than the initial (R_a before 1.28-1.40 μm, R_a after-0,018-0,04 μm, R_z before 7,05-7,890 μm, R_z after 0,126-0,150 μm). Image of 3D surface of the BNDCC composite before grinding process showed the presence of significant inequalities (fig. 20a). After grinding process the surface was completely inequalities (fig. 20b).

http://dx.doi.org/10.5772/59503

a)

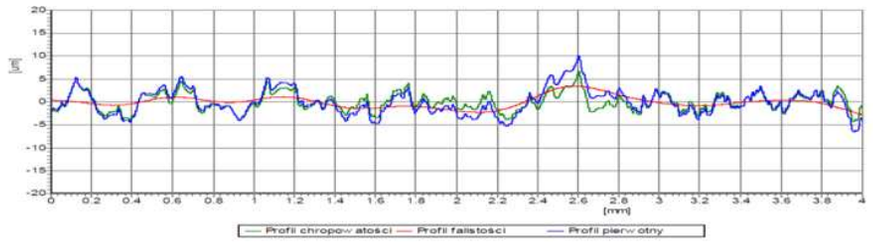

		Średnia	S	Min	Max	Rozstęp
Ra	[µm]	1.248	0.099	1.067	1.655	0.588
Rq	[µm]	1.536	0.112	1.322	1.975	0.652
Rp	[µm]	3.534	0.323	2.903	4.796	1.893
Rv	[µm]	3.556	0.298	2.825	4.220	1.395
Rz	[µm]	7.090	0.517	5.865	8.713	2.848
Rc	[µm]	3.041	0.392	2.482	4.733	2.251
Rt	[µm]	8.811	0.859	6.795	11.061	4.266

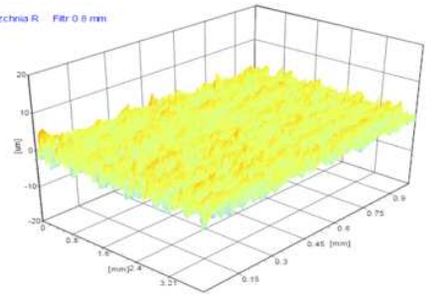

b)

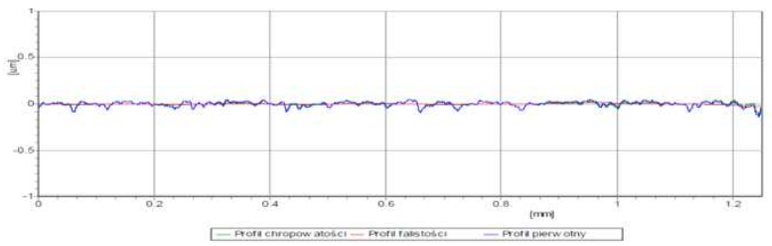

		Średnia	S	Min	Max	Rozstęp
Ra	[µm]	0.018	0.001	0.015	0.022	0.006
Rq	[µm]	0.024	0.002	0.020	0.029	0.009
Rp	[µm]	0.046	0.005	0.037	0.062	0.025
Rv	[µm]	0.080	0.011	0.060	0.122	0.062
Rz	[µm]	0.126	0.014	0.100	0.173	0.073
Rc	[µm]	0.051	0.006	0.039	0.067	0.027
Rt	[µm]	0.171	0.031	0.117	0.247	0.129

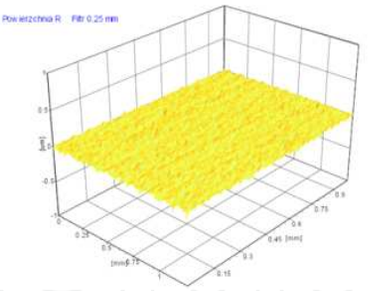

Figure 20. The results of the surface roughness of the composite BNDCC polished 1.47 grinding D25 Ba23: a) before grinding, b) after grinding

2.2.4. The microscopic image of BNDCC composite

The samples of BNDCC composites were observed under a scanning microscope before and after the grinding tests. For all composite samples before grinding process parallel scratches were visible on the surface of the samples. These were probably established through their mechanical treatment after sintering. Microscope image of the samples after grinding showed sharply defined edges with blunted of blade grains in carbide matrix.

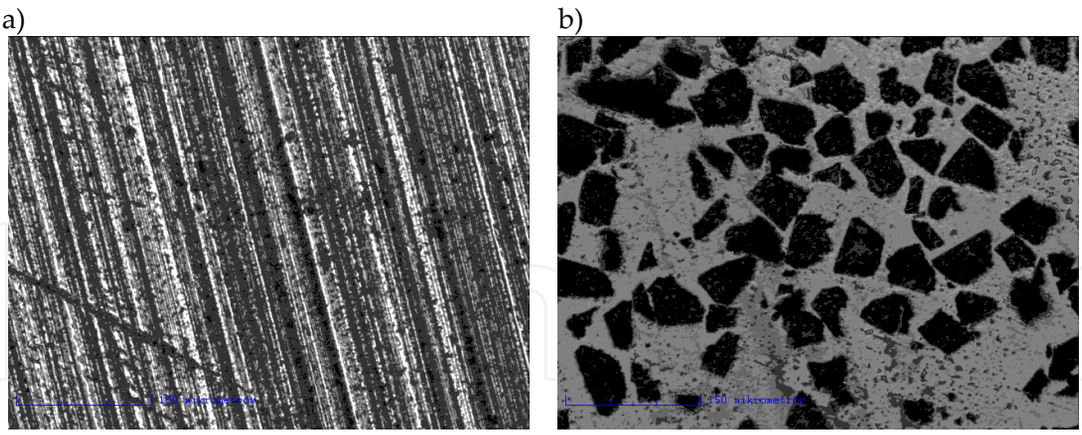

Figure 21. Microscope image of composite BNDCC: a) before; b) after the treatment grinding D46 Ba23 bis binder

2.2.5. The mathematical model of the function of research object

The mathematical model describing the change in the surface roughness Ra of the treated object as a function of the depth of grinding and peripheral speed of grinding wheel was shown in graphic form (fig. 22, 23). The function of the object of research was determined for the grinding process of D46 Ba23 bis wheel and D25W1 wheel BNDCC composite of grit size 4-8 m assuming independent parameters (depth of grinding, ae and grinding wheel peripheral speed vs) and the dependent parameter (surface roughness of the composite). For DOE purposes and analysis of experimental results, STATISTICA was used [15,16]. The range of variability was low. Statistical analysis of the results of experimental studies included

- Approximation of object function tests,
- Statistical verification of the adequacy of the function approximating,
- Statistical verification of significance approximating function coefficients.

The function of the object of research adopted in the form of a polynomial of the second degree of interaction is described by the following formula:

for D25 Ba23 bis

$$y = 0,15 - 7,76\,a_e - 0,01\,V_S + 0,27\,a_e V_S$$

for D25 W1:

$$y = 0,014 - 1,6\,a_e - 0,02\,V_S + 0,18\,a_e V_S \setminus$$

where:

a_e, vs – the size of the input,

$a_0 \div a_5$ – polynomial coefficients.

The results of preliminary calculations showed that the best fit regression equations to the results of the experiment allows the second degree polynomial model of interaction, and

http://dx.doi.org/10.5772/59503

therefore the calculated regression equation stepwise regression presented in this form. Analysis of individual regression equations fit to the experimental results was based on multivariate correlation coefficient R and also based on function values and Student's t-value of F-Snedecor. The level of significance p = 0.05.

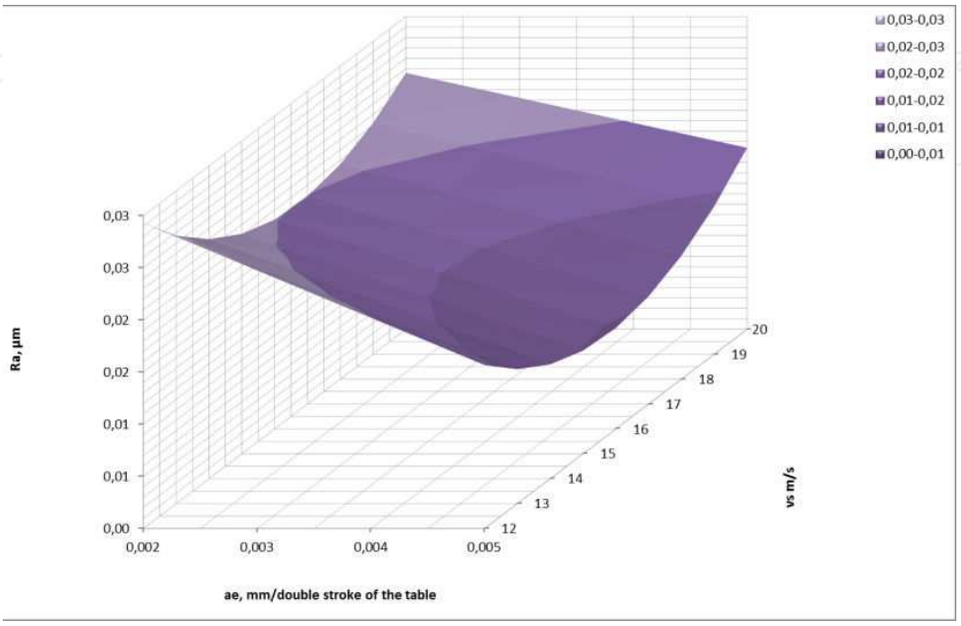

Figure 22. The influence of processing parameters on the surface roughness of the composite samples BNDCC polished by grinding wheel D46 with Ba23 bis

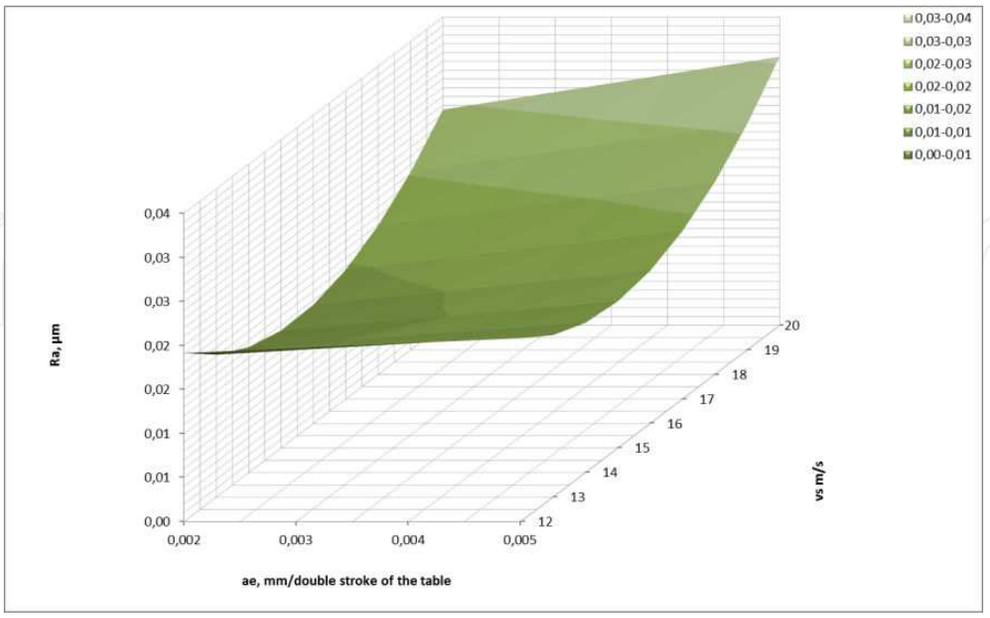

Figure 23. The influence of processing parameters on the surface roughness of the composite samples BNDCC polished by grinding wheel D46 with W1 binder

Analysis of relationship shown in Figure 22 and 23 confirmed that the minimum value of surface roughness BNDCC samples was obtained at the peripheral speed of grinding wheels in the range 14-16 m/s and 0.005 mm depth of grinding/double stroke of table. These data verified the results of performance tests of these samples.

3. Summary and conclusion

Based on the survey it can be concluded that:

- the research glass fulfilled their utility criteria as binders for super hard abrasive tools;
- glass received by frytting method belonged to the group of light glasses (ϱ <2.64 g / cm 3). It was completely transparent with a bluish tint;
- thermodynamic calculation of chemical stability of glass precursors were conducted by VCS algorithm. It was shown in accordance with first assumption that the three compounds were stable in solid states at high temperatures: barium silicate, silicon dioxide, aluminum borosilicate; in the second assumption only one (barium borosilicate). X-ray crystallographic studies have not confirmed the presence of compounds. Investigated samples were in pure amorphous form;
- differential scanning calorimetry of precursor glasses showed their distribution with the separation of water or CO_2 to a temperature of 350°C. The whole sets underwent complete homogenization above 1,350° C;
- substrates were wetted well by all variants of glasses, although in all cases submicrocrystalline sintered corundum was wetted better than silicon carbide. Microscopic observation of samples transverse glass-substrate systems contains submicrocrystalline sintered corundum after the wettability studies showed the presence of narrow interlayer contained barium. In -case of transverse specimens with silicon carbide substrates were much wider, probably resulted from the presence of -silicon in glass and substrate;
- the flexural strength showed the highest values was obtained by W1 and Ba23 bis glass. The work of destruction was tree times lower for W3 glass than W1 glass;
- diamond wheels with D46 or D25 grains and Ba23 bis or W1 binders fulfilled the criteria of utility in the flat grinding process;
- analysis of grinding process efficiency Q_w [x10^{-3}mm^3/s] Q'_w [x10^{-3}mm^3/mm·s], G (listed in Tables 3, 4) showed a very good result under the processing conditions. It was observed that the most favorable results are obtained when the samples of BNDCC composite was machining in – the grinding depth of 0.005 mm/double stroke of table and the peripheral speed of the wheel of 15 m/s;
- the results of the geometrical structure of the surface of the BNDCC composites showed that the grinding surface roughness was R_a 0.018 -0.04 μm compared to the initial roughness of

http://dx.doi.org/10.5772/59503

R_a 1.248 -1.4 μm, R_z after grinding 0.12-136 μm compared to the initial value of R_z 7,096-7,96 μm;

- the mathematical model of grinding process properly describes the working condition necessary to obtain the lowest roughness.

4. Conclusions

- the use of diamond wheels with newly developed vitrified (ceramic) binder in conventional grinding technology has allowed to obtain a mirror of BNDCC composites.

Presented research results were obtained within the project: "Application of modern BNDCC and DDCC composites for cutting tools", Applied Research Program – Contract No. PBS1/A5/7/2012 financed by The National Centre for Research and Development in Poland

Author details

Barbara Staniewicz-Brudnik*, Elżbieta Bączek and Grzegorz Skrabalak

*Address all correspondence to: barbara.brudnik@ios.krakow.pl

Institute of Advanced Manufacturing Technology -011 Kraków, Wroclawska, Poland

References

[1] Kruszewski M, Rosinski M., Grzonka J., Ciupiński Ł., Michalski A., Kurzydłowski K J: Cu composites - a diamond with a high thermal conductivity produced by PPS, Ceramic Materials, 64, 2012, 3, 335-337

[2] Lin K.H, Peng SF, Lin S.T Sintering parameters and wear performances of vitrified bond diamond grinding wheels International Journal of Refractory Metals and Hard Materials, [W] Elsevier, vol 25, 2007, 25-31.

[3] Rosiński M, Chrzanowski W,. Spychalski M, Michalski A. Influence of process parameters on the grinding surface of the composite state WCCo / diamond produced by PPS Ceramic Materials, 64, 2012, 3, 314-318

[4] Rosiński M., Michalski A.: WCCo / cBN composites produced by pulse plasma sintering method, Journal of Materials Science, vol. 47, no 20, pp. 7064-7071, 2012, DOI 10.1007 / s10853-012-x

[5] Rosiński M, Wachowicz J., Ściegienko A., Michalski A. The new composite material is a diamond in the matrix of tungsten carbide for cutting tools for working wood, Ceramic Materials, 64, 2012, 3, 329-332

[6] Staniewicz-Brudnik B.,. Plichta J, Nadolny K., Pluta J.: The study of CBN grinding wheels grinding efficiency with increased porosity of micrograins of spherical corundum. Archive of Production Engineering and Automation, 2006, Vol. 26, No. 2, p. 77-84. Poznan: Poznan University of Technology Publishing House, 2006.

[7] Staniewicz-Brudnik B., Plichta J, Nadolny K.: Effect of porous glass-ceramic materials Addition on the cubic boron nitride (cBN) tools properties. Optica Applicata, 2005, Vol. XXXV, No. 4, p. 809-817., 2005.

[8] Staniewicz-Brudnik B.: grinding with cubic boron nitride ceramic bond. IZTW Bulletin, 2005, No. 1, p. 31-34. Krakow: IZTW, 2006.

[9] Wang Y. et al. Influence of zinc particles on oxidation resistance of diamond / borosilicate glass compositions Diffusion and Defect Data PTB: Solid State Phenomena 175, 2011, 8-12.

[10] Bain Report The Global Diamond Industry

[11] Houy G.: Effect of porosity on the grinding performance of vitrified bond diamond grinding wheels for PCD blades Ceramics International 2012, http: // dx doi.org/ 101016/ceramint.2012304.074

[12] Procyk B, Staniewicz-Brudnik B., Majewska-Albin K.: Investigations of wettability and reactivity in glass / carbon and glass / ceramic systems. [W:] HTC-2000 High Temperature Capillarity, Third International Conference, 19-22 November, Kurashiki, Japan. Transactions of JWRI, 30, 2001, 149-154. [W]: Osaka University: 2001

[13] Jackson M. J., Hitchiner M. P. High Performance Grinding and Advanced Cutting Tools chapter 2 [W]: Springer Science + Business Media New York, 2013.

[14] Partyka J. Sitarz M., Leśniak M., Gasek K., Jeleń P.: The effect of SiO_2/Al_2O_3 ratio on the structure and microstructure of the glasses from SiO_2–Al_2O_3–CaO–MgO–Na_2O–K_2O system Spectrochimica Acta Part A: Molecular and Biomolecular Spectroscopy Volume 134, 5 January 2015, pp.621–630, DOI: 10.1016/j.saa.2014.06.06

[15] Polanski Z.: Optimization methods in machine technology, PWN, Warsaw, 1977

[16] PN – EN 4287